ELSEVIER

Sensors and Actuators A 97–98 (2002) 665–671

SENSORS AND ACTUATORS A PHYSICAL

www.elsevier.com/locate/sna

Active microfluidic mixer and gas bubble filter driven by thermal bubble micropump☆

Jr-Hung Tsai[a,*], Liwei Lin[b]

[a]Department of Mechanical Engineering, University of Michigan, Ann Arbor, MI, USA
[b]Department of Mechanical Engineering, University of California, 5126 Etcheverry Hall, Berkeley, CA 94720-1740, USA

Received 11 June 2001; received in revised form 30 November 2001; accepted 5 December 2001

Abstract

A microfluidic mixer with a gas bubble filter activated by a thermal bubble actuated nozzle-diffuser micropump is successfully demonstrated. The oscillatory flow generated by the micropump can induce wavy interface to increase the contact area of mixing fluids to accelerate the mixing process. The microfluidic mixing channels are 200 μm wide, 50 μm deep and the speed of the mixing liquids are measured at 6.5 μl/min. The optimal mixing result is found when the actuating frequency of thermal bubble reaches 200 Hz. Normalized gray-scale values that correspond to the completeness of the mixing effect are observed to be proportional to the one-third power of the input pulse frequency. Furthermore, a gas bubble filter is integrated and successfully demonstrated in the microfluidic mixing system. A model based on the principle of threshold pressure with respect to the geometry of microchannels is established. © 2002 Published by Elsevier Science B.V.

Keywords: Micropump; Bubble; Microfluidics; Mixing; Filter

1. Introduction

Liquid mixing in the micro-scale presents a great engineering challenge for the success of the micro-total analysis system [1]. In the macro-scale, stirrers or special geometry designs have been used to generate turbulent flow in order to increase the contact area of different mixing liquids to speed up the mixing process. However, it is difficult to generate turbulent flow in microchannels as the flow is in low Reynolds number regime in the micro-scale. Therefore, alternative liquid mixing methods are needed for microfluidic devices. For example, Miyake et al. [2] tried an approach that divides the mixing liquids into tiny drops, mixes the drops separately and collects them together. Deshmukh et al. [3] control the injection of two mixing liquid to be interlaced to accelerate the mixing process.

This paper presents a microfluidic mixing system including a thermal bubble actuated nozzle-diffuser micropump [4], a meander-shape liquid mixing channel and a gas bubble filter. The intrinsically oscillatory flow generated by the bubble actuated nozzle-diffuser micropump and the ''Y-shape'' injection junction can induce a wavy liquid interface to accelerate the mixing process. Furthermore, a gas bubble filter is firstly presented to filter out gas bubbles in microchannels. This filter may have potential applications in microfluidic systems that require no disturbance of gas bubbles.

2. Device structure and fabrication

The microfluidic system is schematically shown in Fig. 1 with two SEM pictures showing the whole system and the close view of the gas bubble filter before the glass cover is bonded with the system. Two liquid inlet ports are designed for the inputs of two types of liquid with one of them passing through the thermal bubble pump that has a pumping chamber of 1 mm in diameter. A meander-shape microchannel with a total length of 10.5 mm (between E and F in Fig. 1), width of 200 μm and depth of 50 μm is designed as the liquid mixing area. The Y-shape injection junction has an opening angle of 40°. The gas bubble filter is placed afterwards and it is composed of 22 fine liquid channels of 10 μm wide and 800 μm long, and a gas bubble channel of 50 μm wide, 1000 μm long as shown in Fig. 1. Gas bubbles will be displaced out of the system from the gas bubble channel to the bubble outlet port such that the liquid outlet port can

☆A portion of this paper was presented in the Transducers'01/Eurosensors XV Conference at Munich, Germany, June 10–14, 2001.

*Corresponding author. Present address: Department of Mechanical Engineering, University of California, 5126 Etcheverry Hall, Berkeley, CA 94720-1740, USA. Tel.: +1-510-642-8983; fax: +1-510-643-5599.
E-mail address: jhtsai@argon.eecs.berkeley.edu (J.-H. Tsai).

0924-4247/02/$ – see front matter © 2002 Published by Elsevier Science B.V.
PII: S0924-4247(02)00031-6

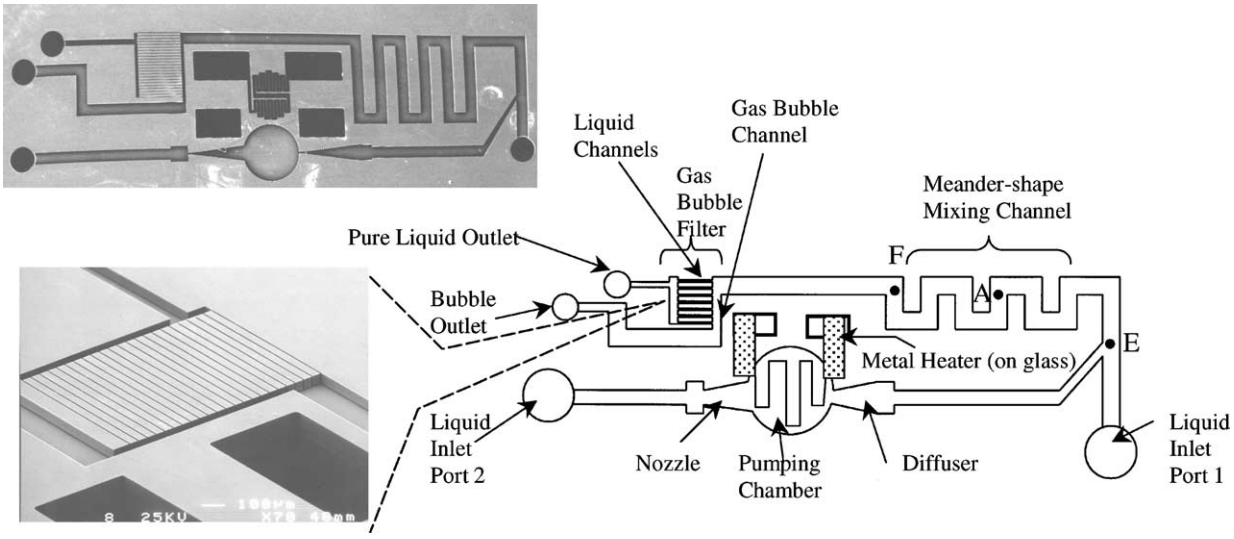

Fig. 1. Schematic drawing of the microfluidic system that includes a nozzle-diffuser-based bubble pump, a meander-shape fluid mixing channel and a gas bubble filter.

deliver bubble-free liquid for downstream sample analyses and tests.

The major fabrication process of the microfluidic system is similar to the thermal bubble actuated micronozzle-diffuser pump [4] as schematically shown in Fig. 2. These features, a micropump, a meander-shape mixing channel, a gas bubble filter and liquid inlet/outlet ports, are fabricated by a two-depth deep reactive ion etching (DRIE) process on a silicon wafer. The two depths are 50 μm for all the fluidic components and 500 μm (through wafer) for the liquid inlet/outlet ports. Its fabrication process starts from thermally growing a 1 μm thick silicon dioxide layer that is patterned and etched as the mask during the 50 μm deep silicon etch. Thereafter, a 9 μm thick photoresist is spun on, patterned and it functions as the mask for the through wafer etching process. After the first DRIE etching process, the photoresist is removed and the silicon oxide mask is used as the second mask to define microfluidic components. After these steps, the silicon wafer is dipped into hydrofluoric acid (HF) to remove silicon dioxide for bonding. The heater used to generate thermal bubbles in the micropump is made of copper (Cu) on the glass wafer. The Pyrex glass wafer is patterned and etched in buffered HF to form recesses for copper heaters to ensure flat bonding surface in the anodic bonding process. Layers of Cr and Cu (20 and 500 nm, respectively) are evaporated and patterned by the lift-off process. Finally, the fabrication process is completed with an anodic bonding of silicon and glass at 380 °C and 1100 V.

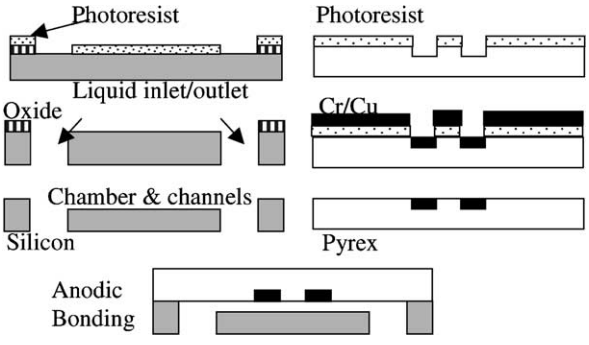

Fig. 2. Simplified fabrication process flow.

3. Microfluidic mixer

3.1. Design principle

In the micro-scale liquid mixing process, the molecular diffusion is the key factor and it can be modeled by Fick's law [5]:

$$J = -AD\frac{\partial C}{\partial x} \tag{1}$$

where J is the flux, A the area, D the diffusion coefficient, C the concentration and x the distance. One can expect that the diffusion flux depends on the diffusion coefficient, concentration gradient and contact surface area. Since diffusion coefficient is a material property and the concentration gradient decays during the mixing process, increasing the contact area is the most convenient approach to accelerate the mixing process. On the other hand, according to Fick's law, the diffusion length between two liquids is proportional to the square root of the multiply of diffusion coefficient and time [5]:

$$l \sim \sqrt{Dt} = \sqrt{\frac{DL}{V}} \tag{2}$$

where l is the diffusion length, t the time, V the flow speed and L the traveling length. Therefore, based on the results from Fick's laws, one way to increase the contact surface

areas is to make the second liquid to oscillate and to penetrate the boundary of the first liquid at point E in Fig. 1 repeatedly as both liquids are moving downstream. This process can shorten the mixing time by introducing more contact areas between two mixing fluids. The nozzle-diffuser-based bubble pump generates oscillatory flow intrinsically, which can be utilized to induce a wavy liquid interface to increase the contact area and to provide intermittent thrust to interlace the liquid supply with the help of the Y-shape fluidic injection junction as shown in Fig. 1.

3.2. Experimental

Flow visualization is often conducted as a qualitative measure of mixing performance. Because the mixing performance is evaluated by the homogeneousness across the global flow field, applying dyes can be an easily accessible flow visualization tool for evaluating the mixing process. Blue food dye and isopropyl alcohol (IPA) are used as the experimental liquids in this mixing experiment. Fig. 3 schematically shows the experimental setup. The blue dye is filled into the microfluidic system firstly from the liquid reservoir through a polyimide tube of 300 μm in diameter to the first liquid inlet port as shown in Fig. 1. IPA is filled into the system in the same way from the second liquid reservoir. The height of the reservoirs of the two liquids are adjusted to about 10 cm above the microfluidic chip to provide a suitable pressure head and a liquid flow rate of around 6.5 μl/min is measured in both fluids. The pressure head is chosen to be higher than that of micropump so that no back flow will be generated from the operation of the thermal bubble pump. Thermal bubbles generate oscillatory flow for IPA to inject into the blue dye in order to enhance the mixing effect.

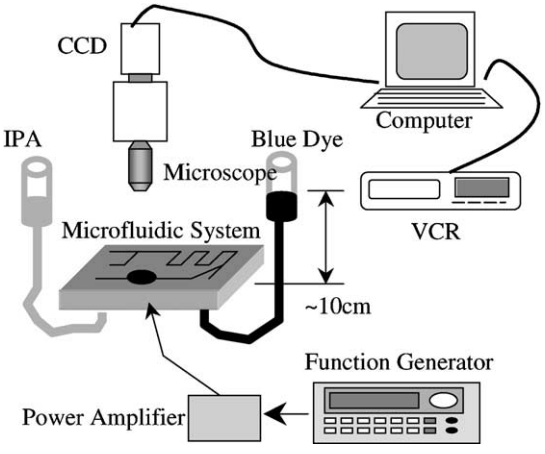

Fig. 3. Schematic drawing of the experimental setup.

3.3. Results and discussion

It is difficult to effectively enhance mixing by merely flowing liquids through a microchannel. Fig. 4 illustrates the experimental result with two liquids, IPA (light color) and the blue dye (dark color) flowing through a meander channel at the speed of around 11 mm/s. The experiment is conducted on a device different from the one shown in Fig. 1 with a gas bubble filter connected to a straight channel. It can be observed that the mixing effect is poor right after the fluidic injection junction at point E. There is no significant color change along the mixing channel in the next 10 mm from point E to F in Fig. 4 and the reason is that the diffusion speed is slower than the flow speed. For example, the diffusion coefficients for most solvents are in the order of 10^{-9} m^2/s [5]; thus the diffusion length is only about 32 μm when the flow speed is 10 mm/s and the traveling distance is 10 mm. Therefore, the mixing result is poor initially and is improved at the end of the meander-shape mixing channel (distance between E and F is 10.5 mm). The mixing effect can be improved by using the bubble actuated nozzle-diffuser micropump as an agitation unit. Fig. 5 shows the agitation effect on the flow pattern by the micropump under a driving frequency of 5 Hz. IPA penetrates into the blue dye flow pattern as the bubble expands in the pumping chamber. When the bubble collapses, the blue dye is sucked back. These motions form a wavy interface between two liquids to increase the contact areas between two liquids and to improve the mixing effect. The mixing results with respect to the micropump driving frequency are shown in Fig. 6. These pictures are taken at point E (the initial mixing point), when the micropump is driven under various pulse frequencies of 5, 50, 100, 150 and 200 Hz. As the micropump driving frequency increases, dense wavy flow pattern is observed. If the wavelength of the wavy flow is equal to or shorter than the diffusion length, the mixing process can

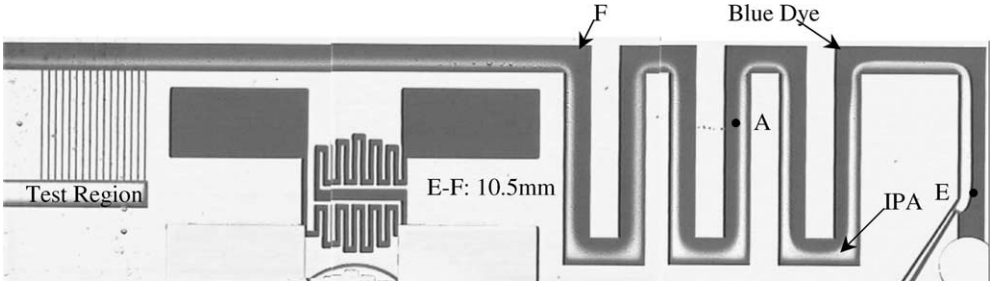

Fig. 4. The diffusion mixing of IPA and the blue dye in the microchannel of 200 μm wide and 50 μm deep without the agitation of micropump.

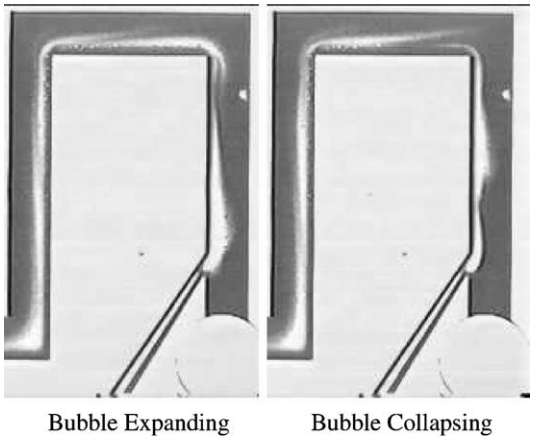

Fig. 5. Wavy liquid interface and interlacing injection effect caused by the micropump agitation at a driving frequency of 5 Hz.

be considered as optimized. Therefore, the minimum frequency to achieve the optimal mixing result under a traveling distance of L is derived in the following equation:

$$\lambda = \frac{V}{f}, \quad f \sim \sqrt{\frac{V^3}{DL}} \tag{3}$$

As shown in Fig. 7, the wave is barely visible as the micropump driving frequency reaches 200 Hz. Based on Eq. (3), this frequency is in the same order of magnitude to achieve optimal mixing effect. The quantitative mixing effects are evaluated by measuring the changes of the gray-scale value of pictures taken at the middle point of the mixing channel (point A in Figs. 1 and 4) and the results are presented in Figs. 7 and 8. Fig. 7 shows the normalized gray-scale value across the mixing channel under different micropump driving frequencies. The abscissa represents the location across the channel. Measured data from the first 30 μm and the last 50 μm across the channel are excluded due to strong error signals from the shadows of the side walls. The vertical axis shows the gray-scale value normalized by the gray-scale value of the pure blue dye. Quantitatively, the normalized gray-scale value at the spot with the coordinate of 150 μm increases from 0.2 to 0.6, 0.75, 0.85

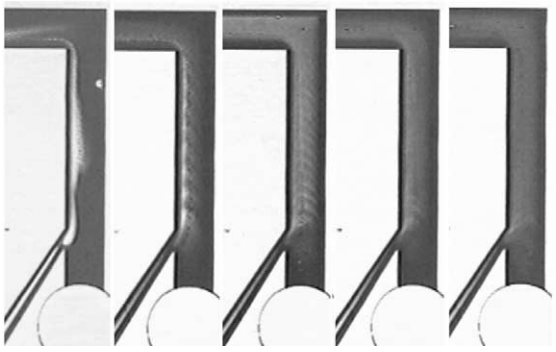

Fig. 6. Mixing of IPA and blue dye near the initial encountering point under various micropump driving frequencies of 5, 50, 100, 150 and 200 Hz from left to right.

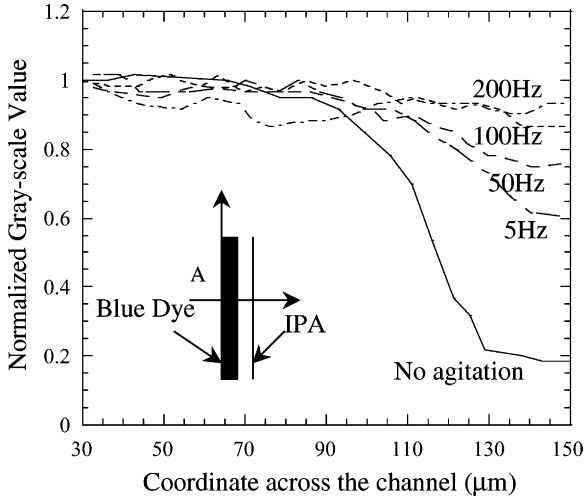

Fig. 7. Normalized gray-scale value across the mixing channel at point A (middle point of microchannel as illustrated in Fig. 4) under various micropump driving frequencies.

and 0.95 when the pumping frequency is increased from 0 to 5, 50, 100 and 200 Hz, respectively. It can be observed that the gray-scale value increases in the IPA flow region with increased pulse frequency. Furthermore, the normalized gray-scale values become more uniform across the channel at higher pulse frequencies. It is noted that the normalized gray-scale value at the blue dye side only changes a little until the pulse frequency reached 200 Hz. One possible reason is that the gray-scale value does not correspond linearly to the concentration changes in the blue dye.

In addition to the mixing effect around the middle of the meander-shape microchannel, the mixing effect downstream as marked as "test region" in Fig. 4 is also characterized. The test region is about 14 mm away from the fluid injection junction. The fine microchannels are connected to one side of the mixing channel to sample the liquid concentration

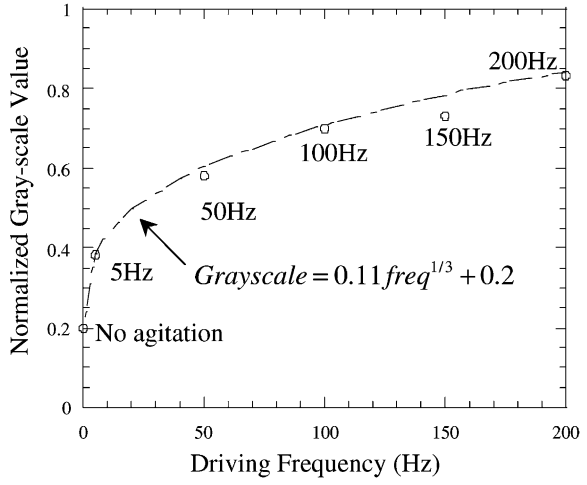

Fig. 8. Normalized gray-scale value of experimental results (shown as the markers) and the curve fitted model (shown as the dashed line) at the test region in Fig. 4 under various micropump driving frequencies.

changes near the wall, where the gray-scale image is more likely to be interfered by the shadow of the wall. In Fig. 8, the normalized gray-scale value at the testing region under various micropump driving frequencies is plotted. It is found that the gray-scale value increases proportionally to the one-third power of the pulse frequency. According to the trend of the fitted curve, the gray-scale value increases slowly at higher pulse frequency. This is predicted as mentioned previously that once the wavelength of the wavy flow is shorter than the diffusion length, the mixing process is optimized.

4. Gas bubble filter

4.1. Principle

The working principle of the gas bubble filter is based on the fact that the surface energy of the gas bubble increases when it is forced to move into a narrower channel as illustrated in Fig. 9. A certain amount of energy is required to deform the bubble. If the geometry of the bubble is assumed as a two-dimensional shape, the surface energy difference of the gas bubble between state A and B can be expressed as

$$\mathrm{d}E = \gamma_{\mathrm{lg}}\, 2(h+w)\,\mathrm{d}s_2 - \gamma_{\mathrm{lg}}\, 2(h+W)\,\mathrm{d}s_1 \tag{4}$$

where E is the surface energy, γ_{lg} the surface energy per unit area between liquid and gas, h the depth of the channel, w the width of the narrower channel, W the width of the wider channel and s is a tiny displacement. The volume variations will be equal as the result of mass conservation, if the density variation of the bubble is negligible:

$$hw\,\mathrm{d}s_2 = hW\,\mathrm{d}s_1 \tag{5}$$

Hence, the surface energy difference equation can be rearranged as

$$\mathrm{d}E = 2\gamma_{\mathrm{lg}}\, h\left(\frac{W}{w} - 1\right)\mathrm{d}s_1 \tag{6}$$

On the other hand, the work required to transform the gas bubble from state A to B is

$$\mathrm{d}K = P_1 hW\,\mathrm{d}s_1 - P_2 hw\,\mathrm{d}s_2 \tag{7}$$

where K is the work and P the pressure. The surface energy difference is equal to the work required between the states A and B and the pressure difference is derived as

$$P_1 - P_2 = 2\gamma_{\mathrm{lg}}\left(\frac{1}{w} - \frac{1}{W}\right) \tag{8}$$

According to Eq. (8), a gas bubble filter can be designed by constructing the right combinations of the narrow and wide microchannel dimensions.

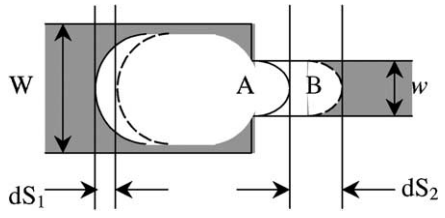

Fig. 9. Schematic drawing of the gas bubble deformation into a narrow channel.

4.2. Experiments and results

The proposed gas bubble filter is demonstrated by connecting an input channel of 200 μm wide to a group of fine liquid output channels of 10 μm wide and a gas bubble output channel of 50 μm wide as shown in Fig. 10. The fine channels are designed as a group instead of using a single fine channel design in order to average out the output of bubble-free liquid. By using IPA as the working liquid, the operation of the gas bubble filter is demonstrated in the series of optical pictures shown in Fig. 10. The fine microchannels have a higher threshold pressure than the gas bubble channel such that gas bubbles pass through the gas bubble channel without entering the fine liquid output channel as shown in Fig. 10(a)–(c). If the diameters of gas bubbles are smaller than the width of the fine liquid output channel or the flow pressure is higher than the threshold pressure of the fine liquid channel, the bubble can flow into the fine liquid output channels. The surface energy per unit area for IPA is about 22 mJ/m^2 [6] and the threshold pressure for the fine liquid channel and the gas bubble channel are calculated as 4.18 kPa and 660 Pa, respectively. Therefore, as long as the pressure is between 600 Pa and 4.18 kPa, the gas bubble filter will be functioned properly. If the applied pressure is less than 660 Pa, the gas bubble will be accumulated at the input channel site and will not even pass the gas bubble channel as predicted by Eq. (8). This phenomenon is observed in experiments when the micropump is operated with low pressure head. On the other hand, when the micropump is operated to generate a sudden burst of bubble to generate high pressure head, gas bubbles have been observed to be squeezed into the fine liquid channels.

Overall, the micromixer and the gas bubble filter worked as planned. Several issues require further investigations. First, the bubble actuated micropump worked as an agitation unit in the mixing experiments such that mixing process is determined primarily on the oscillatory flow patterns generated by the thermal bubbles and not the pumping results from the bubble pump. It will be important to characterize the mixing effects when one or two fluids are powered directly from the bubble pump. Second, the Y-shape injection junction design has an opening angle of 40°. Since the injection angle as well as the opening geometry can change the patterns of the wavy flow drastically and affect the mixing process, the optimal injection junction design requires careful studies and this may involve fluidic analyses and simulations. Third, the pressure head that can be

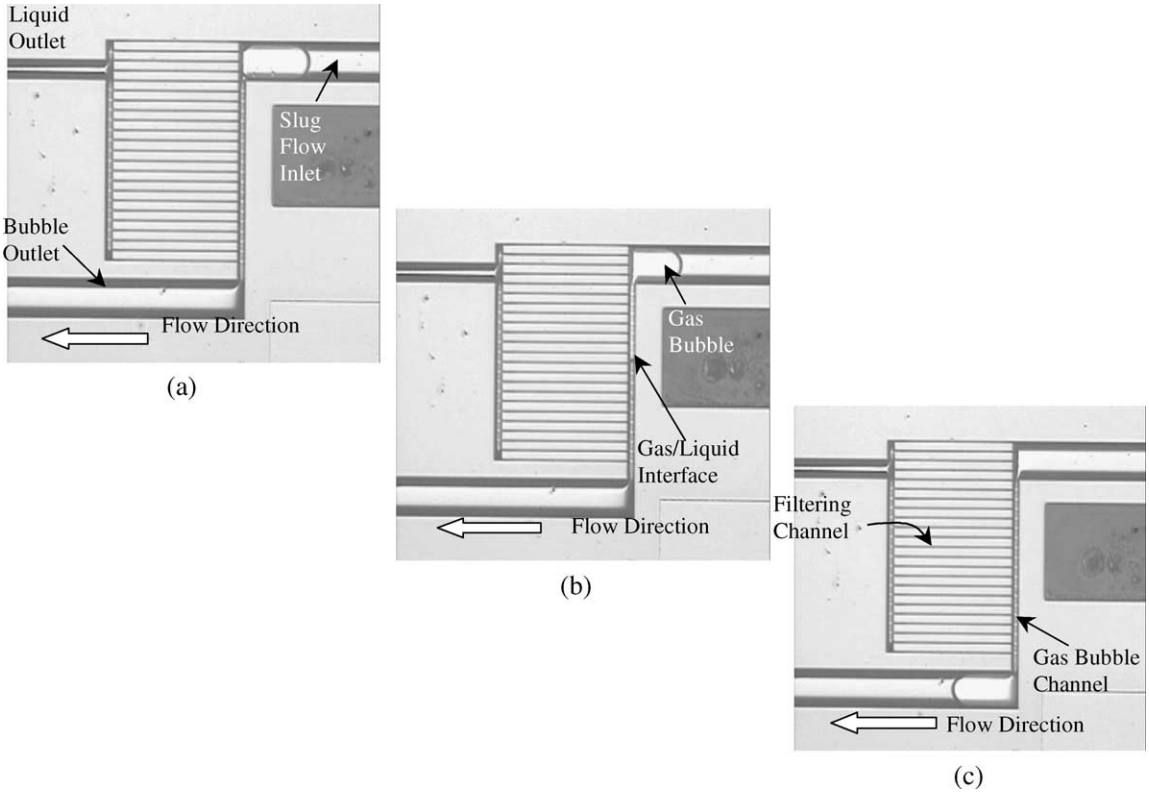

Fig. 10. Sequential pictures of the gas bubble filter in operation actuated by the nozzle-diffuser bubble pump: (a) gas bubble reaching the filter; (b) bubble filtered into the gas bubble channel; (c) bubble separation from liquid outlet.

generated by using different sizes and types of thermal bubble pumps will also be an important factor to generate wavy flow for mixing and should be investigated. Fourth, the flow speeds of the two mixing liquids, the types of mixing liquids and possible temperature effects are other issues to be explored further. On the gas bubble filter part, it is important to study the surface effects of the microchannel. For example, in the simplified model developed in this work, the side walls of the microchannel are drawn as hydrophilic and it will be important to study the gas bubble filtering effects if some or all of the walls are hydrophobic.

5. Summary

This paper has demonstrated a microfluidic mixing system with a gas bubble filter based on the thermal bubble agitation mechanism. The intrinsically oscillatory flow generated by the thermal bubbles enhance the mixing process. The mixing effect with bubble driving pulse frequencies from 0 to 200 Hz is studied. It is found that dense fluidic waves generated by the oscillatory flow accelerate the mixing process. When the wavelength of the wavy flow is shorter than the theoretical diffusion length, the optimal mixing effect is achieved. Furthermore, a gas bubble filter is proposed, fabricated and successfully demonstrated with the microfluidic mixer. A simple model is developed to estimate the required pressure thresholds in the design of the gas bubble filter.

Acknowledgements

The authors thank Prof. Liepmann's research group at University of California, Berkeley, for valuable discussions and the microlab staff at University of California, Berkeley, for the help in the microfabrication processes. This work is supported in part by an NSF career award (ECS-0096098) and a DARPA/MTO/MEMS grant.

References

[1] A. Manz, N. Graber, H.M. Widmer, Miniaturized total chemical analysis systems: a novel concept for chemical sensing, Sens. Actuators B 1 (1990) 244–248.
[2] R. Miyake, T.S. Lammerink, M. Elwenspoek, J. Fluitman, Micromixer with fast diffusion, in: Proceedings of the 1993 IEEE Micro-electromechanical Systems Workshop, Orlando, FL, 1999, pp. 141–146.
[3] A.D. Deshmukh, D. Liepmann, A.P. Pisano, Continuous micromixer with pulsatile micropumps, in: Proceedings of the IEEE Solid-state Sensor and Actuator Workshop, Hilton Head Island, SC, 2000, pp. 73–76.
[4] J.H. Tsai, L. Lin, A thermal bubble actuated micronozzle-diffuser pump, in: Proceedings of the 2001 IEEE Micro-electromechanical Systems Workshop, Interlaken, Switzerland, 2001, pp. 409–412.

[5] E.L. Cussler, Diffusion: Mass Transfer in Fluid Systems, Cambridge University Press, Cambridge, 1984.
[6] N.B. Vargaftik, Tables on the Thermophysical Properties of Liquids and Gases, Hemisphere, Washington, DC, 1975, pp. 418–420.

Biographies

Jr-Hung Tsai received MS in mechanical engineering from the National Tsing Hua University, Taiwan, in 1994. In 2001, he received his PhD in mechanical engineering from University of Michigan, USA. Now he is a research engineer in Kumetrix, Inc., in researching and developing micro-biodiagnosis devices. His research interests are mainly in design, modeling and fabrication of microfluidic devices for biomedical and bioanalytical applications.

Liwei Lin received his MS and PhD in mechanical engineering from the University of California, Berkeley, in 1991 and 1993, respectively. He joined BEI Electronics, Inc., USA, from 1993 to 1994 in research and development of microsensors. From 1994 to 1996, he was an Associate Professor in the Institute of Applied Mechanics, National Taiwan University, Taiwan. From 1996 to 1999, he was an Assistant Professor at the Mechanical Engineering and Applied Mechanics Department at the University of Michigan. He joined the University of California at Berkeley in 1999 and is now an Associate Professor at Mechanical Engineering Department and Co-Director at Berkeley Sensor and Actuator Center, NSF/Industry/University Research Cooperative Center. His research interests are in design, modeling and fabrication of microstructures, microsensors and microactuators as well as mechanical issues in micro-electromechanical systems including heat transfer, solid/fluid mechanics and dynamics. He is the recipient of the 1998 NSF career award for research in MEMS Packaging and the 1999 ASME Journal of Heat Transfer best paper award for his work on micro-scale bubble formation. He led the effort in establishing the MEMS sub-division in ASME and is currently serving as the Vice Chairman of the Executive Committee for the MEMS sub-division. He holds seven US patents in the area of MEMS.